Int. J. Heat Mass Transfer. Vol. 11, pp. 27–38. Pergamon Press 1968. Printed in Great Britain

TRANSIENT HEAT TRANSFER FOR FORCED CONVECTION FLOW OVER A FLAT PLATE OF APPRECIABLE THERMAL CAPACITY AND CONTAINING AN EXPONENTIAL TIME-DEPENDENT HEAT SOURCE

MOUSTAFA SOLIMAN* and HAROLD A. JOHNSON†

(*Received* 19 *January* 1967)

Abstract—Experimental data and theoretical predictions are presented for the transient mean wall temperature of a flat plate of appreciable thermal capacity, heated by an exponential heat source [q_0 exp (t/t_0)] and cooled on both sides by a steady, incompressible, forced convection flow with a Prandtl number around unity. Within the range of these data, the parameter $Z_L/t_0 = L/u_\infty t_0$ is a sufficient criterion to conclude that: for $0{\cdot}28 \leqslant Z_L/t_0 \leqslant 2$ a turbulent flow solution is in agreement with the data; for $5 \leqslant Z_L/t_0 < \infty$ the Chambré solution (slug flow) agrees well with the data; and for $2 < Z_L/t_0 < 5$ a semi-empirical correlation is developed which satisfactorily predicts the wall temperature.

NOMENCLATURE

B, $= H\sqrt{(\kappa)}/K$;
b, thickness of the plate;
c, specific heat;
H, $= \frac{1}{2}\rho_w c_w b$, half of the ribbon thermal capacity;
h_m, mean heat-transfer coefficient for a plate of appreciable thermal capacity;
$h_{m,0}$, mean heat-transfer coefficient for a plate of zero thermal capacity;
I, function related to the incomplete gamma function and defined in [7], see equation (13);
K, thermal conductivity of the fluid;
L, length of the plate;
q_0, initial step in the rate of heat generation inside the plate per unit surface area of the plate;
q_{net}, net heat flux from the wall, see equation (5a);
Re_L, $= u_\infty L/\nu$, Reynolds number;
S, $= B^2/t_0$, dimensionless thermal capacity parameter;
T, temperature rise over that at infinity;
T_R, $= [q_0\sqrt{(\kappa t_0)}/K]$, reference temperature;
t, time;
t_0, period of the exponential heat source;
u, velocity component parallel to the wall;
v, velocity component perpendicular to the wall;
x, distance along the wall;
y, distance normal to the wall;
z, x/u_∞ or $= x/u_m$.

Greek symbols
Γ, incomplete gamma function;
ϵ_H, thermal eddy diffusivity;
ζ, dummy variable;
κ, thermal diffusivity of the fluid;
λ, dummy variable;
ν, kinematic viscosity of the fluid;
ρ, density;
σ, $= \nu/\kappa$, Prandtl number;
ϕ, dimensionless heat source function;

* Preliminary Design Department, AiResearch Manufacturing Company, Los Angeles, California.
† Professor of Mechanical Engineering, University of California, Berkeley.

ψ, defined in equation (13).

Subscripts

∞, refers to conditions far from the wall;
L, means that the parameter is evaluated using the heated length of the plate L;
m, refers to an average value over the heated length L;
$m, 0$, refers to an average value in case the plate is of zero thermal capacity;
w, refers to conditions at the wall.

INTRODUCTION

TRANSIENT convection heat transfer has frequently been a topic of discussion. In a previous paper [1], the authors presented an approximate analysis, with experimental data, for the transient mean wall temperature of a flat plate of appreciable thermal capacity. The plate was heated by a step increase in the heat generation rate and was cooled on both sides by a steady, incompressible, turbulent flow of water with a Prandtl number of unity. Theoretical and experimental data agreed over a range of Reynolds numbers $5 \times 10^5 \leqslant Re_L \leqslant 2 \times 10^6$. This paper extends the analysis of [1] to accommodate the condition in which the plate is heated by an exponential time-dependent heat source $[q_0 \exp(t/t_0)]$. The analytical results are then compared to experimental data obtained with water as the flow medium.

A survey of the current literature in the area of transient forced-convection heat transfer can be found in [2].

This study is based on the same three analytical models used in [1], slug flow, turbulent boundary-layer flow, and quasi steady-state (constant heat-transfer coefficient) models. Each of the three analyses is valid in a different range that is established after the experimental and analytical data are compared and is dependent upon the flow velocity and the period of the exponential heat source (t_0).

ANALYTICAL MODELS

Slug flow model

In the slug flow model (Chambré [4] and Johnson and Chambré [3]), fluid passes tangentially over the surface of a flat plate with a uniform, steady-state velocity distribution. If (1) conduction effects in the flow direction are ignored, (2) fluid properties are assumed constant, and (3) viscous dissipation is neglected, then the fluid temperature distribution obeys the following equation (see Fig. 1):

$$\frac{\partial T}{\partial t} + u_m \frac{\partial T}{\partial x} = \kappa \frac{\partial^2 T}{\partial y^2}, \quad t > 0, \quad x > 0, \quad y > 0. \qquad (1)$$

The plate, initially at the ambient fluid temperature T_0 is heated by a uniform internal heat

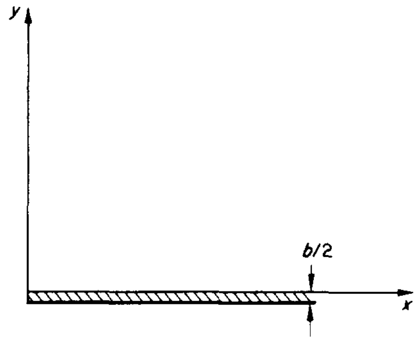

FIG. 1. Physical model and coordinates.

source per unit of heat-transfer area $[q_0 \exp (t/t_0)]$. The plate has a thermal capacity per unit of heat-transfer area $H = (\rho_w c_w b/2)$ but negligible thermal resistance (i.e. at any instant the wall temperature is assumed constant over the thickness b). Hence, the side conditions are

$$T(0, x, y) = 0, \quad x > 0, \quad y > 0; \quad T(t, 0, y) = 0, \quad t > 0, \quad y > 0 \qquad (2)$$

$$T(t, x, \infty) = 0, \quad t > 0, \quad x > 0;$$
$$-K \frac{\partial T}{\partial y}(t, x, 0) = q_0 \exp(t/t_0) - H \frac{\partial T}{\partial t}(t, x, 0), \quad t > 0, \quad x > 0. \qquad (3)$$

The system of equations (1–3) was solved by Chambré [3] by means of double Laplace transformation methods. Expressions, tables, and charts are given in [4] for the local and mean wall temperatures.

Turbulent boundary-layer model

The transient energy equation for plain, incompressible, turbulent boundary-layer flow over a flat plate is

$$\frac{\partial T}{\partial t} + u(x,y)\frac{\partial T}{\partial x} + v(x,y)\frac{\partial T}{\partial y} = \frac{\partial}{\partial y}\left[(\kappa + \epsilon_H)\frac{\partial T}{\partial y}\right],$$
$$t > 0, \quad x > 0, \quad y > 0. \qquad (4)$$

In writing equation (4), the diffusion in the x-direction and the viscous dissipation have been neglected, and the fluid properties are assumed constant. As with the slug flow model, the plate is assumed to have a thermal capacity H and zero thermal resistance. The side conditions in equation (2) and the first condition in equation (3) remain unchanged while the second condition in equation (3) may be written as

$$\lim_{y\to 0}\left[-\rho c(\kappa + \epsilon_H)\frac{\partial T}{\partial y}\right] = q_0 \exp(t/t_0) - H\frac{\partial T}{\partial y}(t, x, 0), \quad t > 0, \quad x > 0. \qquad (5)$$

Assuming, as in [1] that, (1) the velocity components (u, v) and the eddy diffusivity for heat ϵ_H are independent of time, (2) the eddy diffusivity for heat equals the eddy diffusivity for momentum, (3) the Prandtl number is unity, (4) the shear stress is invariable across the boundary layer, and (5) a $\frac{1}{7}$th power law exists for the velocity profile and a wall shear stress as derived from this profile, (see [1, 5]), then the transport term is obtained as

$$\kappa + \epsilon_H = 0{\cdot}179\, u_\infty^{27/35}\, \nu^{8/35}\, x^{-3/35}\, y^{6/7}. \qquad (6)$$

An approximate solution describing the mean wall temperature for the above problem, except that the plate was heated by a step heat source q_0, was obtained and tested against experimental data given in [1]. This solution was derived by first considering a plate of zero thermal capacity ($H = 0$) and then joining the small times solution of equation (4) (one dimensional diffusion) with the steady-state solution at $t = x/u_\infty$. When this solution was integrated along the length of the plate (L), equations (31) and (32) in [1] resulted; they are rearranged here to give ($\sigma = 1$)

$$\frac{T_{m,0}K}{q_0\sqrt{\kappa}} = \frac{Z_L^{0\cdot 2}}{(u_\infty^2/\kappa)^{0\cdot 3}}\left[28{\cdot}19\,(t/Z_L)^{0\cdot 125} - 2{\cdot}94\,(t/Z_L)^{1\cdot 2}\right], \quad t \leqslant Z_L \qquad (7)$$

$$\frac{T_{m,0}K}{q_0\sqrt{\kappa}} = \frac{25{\cdot}25\, Z_L^{0\cdot 2}}{(u_\infty^2/\kappa)^{0\cdot 3}}, \quad t \geqslant Z_L. \qquad (8)$$

Equations (7) and (8) will be used to extend the solution of [1] to arbitrary time-dependent heat sources, of which the exponential function is of primary interest.

1. *Case of zero thermal capacity* [$H = 0$ *in equation* (5)]

Since the energy equation (4) is linear, the wall temperature response to an arbitrary time-dependent heat source [$q(t) = q_0\,\phi(t)$] can be obtained from the step solution of equations (7) and (8) by using the Duhamel's integral, [6]. Hence,

$$T_{m,0} = \frac{q_0(\sqrt{\kappa})\, Z_L^{0\cdot 2}}{K(u_\infty^2/\kappa)^{0\cdot 3}}\left\{\int_0^t \left[28{\cdot}19\left(\frac{t-\lambda}{Z_L}\right)^{0\cdot 125} - 2{\cdot}94\left(\frac{t-\lambda}{Z_L}\right)^{1\cdot 2}\right]\cdot\frac{\mathrm{d}\phi(\lambda)}{\mathrm{d}\lambda}\mathrm{d}\lambda + \left[28{\cdot}19\left(\frac{t}{Z_L}\right)^{0\cdot 125} - 2{\cdot}94\left(\frac{t}{Z_L}\right)^{1\cdot 2}\right]\phi(0)\right\}, \quad t \leqslant Z_L \qquad (9)$$

$$T_{m,0} = \frac{q_0(\sqrt{\kappa})\, Z_L^{0\cdot 2}}{K(u_\infty^2/\kappa)^{0\cdot 3}}\left\{\int_{t-Z_L}^t \left[28{\cdot}19\left(\frac{t-\lambda}{Z_L}\right)^{0\cdot 125} - 2{\cdot}94\left(\frac{t-\lambda}{Z_L}\right)^{1\cdot 2}\right]\times\frac{\mathrm{d}\phi(\lambda)}{\mathrm{d}\lambda}\mathrm{d}\lambda + 25{\cdot}25\,\phi(t - Z_L)\right\}, \quad t \geqslant Z_L \qquad (10)$$

Carrying out the integrals in equations (9) and

(10) by parts and substituting $\phi(t) = \exp(t/t_0)$ results in ($\sigma = 1$).

$$\frac{T_{m,0}}{T_R} = \exp(t/t_0)\,\psi(t/t_0), \qquad t/t_0 \leqslant Z_L/t_0 \qquad (11)$$

$$\frac{T_{m,0}}{T_R} = \exp(t/t_0)\,\psi(t/t_0 = Z_L/t_0), \qquad t/t_0 \geqslant Z_L/t_0 \qquad (12)$$

where

$$\psi(t/t_0) = \frac{1}{(Z_L/t_0)(t_0 u_\infty^2/\kappa)^{0\cdot 3}} \left\{28\cdot 5 \int_0^{t/t_0} (Z/t_0)^{0\cdot 075} \,.\, I(2\cdot 83\, Z/t_0, -\tfrac{7}{8})\, \mathrm{d}Z/t_0 + 26\cdot 5\, I(2\cdot 83\, t/t_0, -\tfrac{7}{8}) \left[(Z_L/t_0)^{1\cdot 075} - (t/t_0)^{1\cdot 075}\right]\right\} \qquad (13)$$

and

$$I(X, -\tfrac{7}{8}) = \frac{\int_0^{X/\sqrt{8}} \zeta^{-\frac{7}{8}} \exp(-\zeta)\, \mathrm{d}\zeta}{\Gamma(\frac{1}{8})}. \qquad (14)$$

The function I is tabulated in [7].

The instantaneous mean heat-transfer coefficient for a wall of zero thermal capacity $h_{m,0}(t)$ is defined as the ratio of the heat flux at the wall (which is equal to the heat source in this case) to the mean wall temperature. The expressions for $h_{m,0}(t)$, as obtained from equations (11) and (12), are ($\sigma = 1$)

$$\frac{h_{m,0}(t)\sqrt{(\kappa t_0)}}{K} = \frac{1}{\psi(t/t_0)}, \quad t/t_0 \leqslant Z_L/t_0 \qquad (11a)$$

$$\frac{h_{m,0}(t)\sqrt{(\kappa t_0)}}{K} = \frac{1}{\psi(t/t_0 = Z_L/t_0)}, \quad t/t_0 \geqslant Z_L/t_0 \qquad (12a)$$

2. *Case of finite thermal capacity*

In this case, the plate is treated as a lumped capacity containing an exponential heat source. An energy balance at the wall neglecting conduction in the chordwise direction results in

$$q_{\text{net},m} = q_0 \exp(t/t_0) - H\frac{\partial T_m}{\partial t}. \qquad (5a)$$

The mean net heat flux from the wall $q_{\text{net},m}$ may also be written as

$$q_{\text{net},m} = h_m(t)\, T_m \qquad (5b)$$

where h_m and T_m are the mean heat-transfer coefficient and wall temperature, respectively, for a wall of appreciable thermal capacity. Both h_m and T_m as well as q_{net} are unknown. Eliminating $q_{\text{net},m}$ between equations (5a) and (5b), one gets

$$\frac{\mathrm{d}T_m}{\mathrm{d}t} + \frac{h_m(t)}{H} T_m = \frac{q_0 \exp(t/t_0)}{H}. \qquad (5c)$$

In order to solve equation (5c), it is assumed that $h_m(t) = h_{m,0}(t)$, i.e. the effect of the wall thermal capacity on the values of the heat-transfer coefficient is negligible. The same assumption was used in [1], and the wall temperatures obtained were in good agreement with the experimental data. Moreover, this method was tested for the slug flow model, in [2], and the wall temperatures agreed with Chambré's solution given in [4]. These results are not surprising if one examines the effect of wall thermal capacity on the heat-transfer coefficient as revealed by the experimental data in [1] and as shown in Fig. 17. Substituting for $h_m(t)$ in equation (5c) from equations (11a) and (12a) results in two first-order differential equations whose solutions are ($\sigma = 1$).

$$T_m/T_R = \frac{1}{\sqrt{S}} \exp\left[-\frac{1}{\sqrt{S}}\int_0^{t/t_0} \frac{\mathrm{d}t'/t_0}{\psi(t'/t_0)}\right] \int_0^{t/t_0} \exp\left[t'/t_0 + \frac{1}{\sqrt{S}}\int_0^{t'/t_0} \frac{\mathrm{d}t''/t_0}{\psi(t''/t_0)}\right] \mathrm{d}t'/t_0, \quad t/t_0 \leqslant Z_L/t_0 \qquad (15)$$

$$T_m/T_R = \frac{1}{\sqrt{S}} \exp - \left[\frac{t/t_0 - Z_L/t_0}{(\sqrt{S})\,\psi(t/t_0 = Z_L/t_0)} + \frac{1}{\sqrt{S}}\right.$$

$$\times\int_0^{Z_L/t_0}\frac{\mathrm{d}t'/t_0}{\psi(t'/t_0)}\Bigg]\int_0^{Z_L/t_0}\exp\left[t'/t_0+\frac{1}{\sqrt{S}}\int_0^{t'/t_0}\frac{\mathrm{d}t''/t_0}{\psi(t''/t_0)}\right]\mathrm{d}t'/t_0$$
$$+\frac{\psi(t/t_0=Z_L/t_0)}{[1+(\sqrt{S})\,\psi(t/t_0=Z_L/t_0)]}\left\{\exp(t/t_0)-\exp\left[Z_L/t_0-\frac{(t/t_0-Z_L/t_0)}{(\sqrt{S})\,\psi(t/t_0=Z_L/t_0)}\right]\right\},\quad t/t_0\geqslant Z_L/t_0. \tag{16}$$

The numerical evaluation of the integrals appearing in equations (15) and (16) is time-consuming because of the complex form of the function ψ. As a result computers may be used. However, over the range of values of Z_L/t_0 reported in the experimental data and for $t/t_0 > 0{\cdot}5$, ψ can be approximated by

$$\psi(t/t_0)\simeq\frac{26{\cdot}5\,(Z_L/t_0)^{0{\cdot}075}}{(t_0\,u_\infty^2/\kappa)^{0{\cdot}3}}\,I(2{\cdot}83\,t/t_0,-\tfrac{7}{8}). \tag{17}$$

The error introduced in T_m/T_R by using the above approximate form for ψ was found to be less than 5 percent [2].

Steady-state heat-transfer coefficient model

In this case, the plate is again treated as a lumped capacity containing an exponential heat source, but having a steady-state heat-transfer coefficient h_m on both sides. The value of h_m which is used in equation (5c) can be written from equation (8) as ($\sigma = 1$).

$$h_m = 0{\cdot}0396\,\frac{K}{L}\left(\frac{u_\infty L}{\nu}\right)^{0{\cdot}8} \tag{8a}$$

After integrating equation (5c) and substituting for h_m from equation (8a), the value for the dimensionless mean wall temperature is

EXPERIMENTAL MEASUREMENTS

The flat plate is simulated by a thin Deltamax (50% nickel, 50% iron) ribbon, 0·125-in wide and 3-in long, and either 0·004-in or 0·014-in thick soldered onto heavy terminal brass blocks and vertically suspended along the centerline of a $\frac{7}{8}$ by $\frac{3}{8}$-in test section (see Fig. 2). Energy is generated in the ribbon by an electric current which is supplied by a set of storage batteries and is controlled by a transient power generator developed at the Oak Ridge National Laboratory (see [8] and [2]). This generator consists of 100 thyratron tubes connected in parallel. These tubes (i.e. switches), in conjunction with a sweep signal generator which is adjustable and which triggers the thyratron switches, are scheduled to produce a smoothly rising exponential function for the power in the plate $[q_0\exp(t/t_0)]$. By changing the value of the sweep time, different values for the period of the exponential (t_0) are obtained. The ribbon is cooled on both sides by a steady flow of deionized, de-aerated water. During most of the tests, the temperature of the water in the test section T_0, which is also the initial temperature of the plate, is kept at approximately 270°F (the Prandtl number is, then, approximately unity), and the pressure of the water is maintained at approximately 800

$$T_m/T_R=\frac{\left\{\exp(t/t_0)-\exp\left[-0{\cdot}0396\,\dfrac{(t_0u_\infty^2/\kappa)^{0{\cdot}3}\,(t/t_0)}{(\sqrt{S})\,(Z_L/t_0)^{0{\cdot}2}}\right]\right\}}{\left\{(\sqrt{S})+\dfrac{0{\cdot}0396\,(t_0u_\infty^2/\kappa)^{0{\cdot}3}}{(Z_L/t_0)^{0{\cdot}2}}\right\}} \tag{18}$$

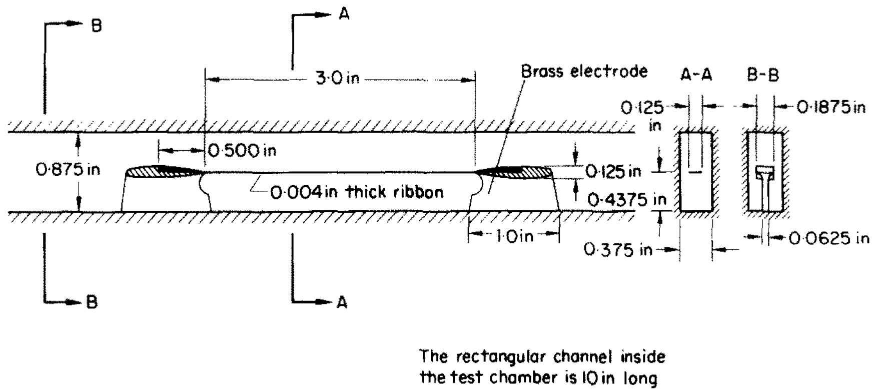

FIG. 2. Sketch of the flow channel and ribbon mounting arrangement in high pressure visual test chambers.

psia. To prevent boiling on the surface of the ribbon, a special device is used to cut off the power if the ribbon temperature reaches 420°F which is about 100°F below the saturation temperature of the circulating water. In the present scheme, the ribbon also serves as a resistance thermometer; ribbon voltage and current are measured to determine the mean wall temperature and the amount of heat generated by the ribbon. The voltages across the ribbon and across a precise current shunt are both displayed on precision 10 by 10 cm screen grids of two Tektronix dual-beam oscilloscopes, types 502 and 561A, and photographed by two polaroid oscilloscope cameras. The more pronounced the deflection recorded on the scope screen, the higher the accuracy of the measurement. Therefore, the small times measurements, i.e. when the voltages are relatively small, are displayed on the whole screen of one scope, whereas the other scope records voltages over the entire time interval. In this way, the probable error in the mean wall temperature is estimated to be 10–5 degF, depending on whether the time is small or large, respectively. The test conditions are listed in Table 1.

Table 1. Test conditions

Figure No.	Thickness of ribbon b (in)	Half the thermal capacity of the ribbon $H = \frac{1}{2}\rho_w c_w b$ (Btu/ft² °F)	$B^2 = (H^2\kappa/K)$ (ms)	Initial step q_0 (Btu/h ft²)	Period of exponential t_0 (ms)	Initial* temperature T_0 (°F)	Velocity u_m (ft/s)
3	0·004	0·01	15·6	16493	48·5	275	14
3	0·004	0·01	15·6	16600	50·1	271	8
4	0·004	0·01	15·6	16546	16·4	273	14
4	0·004	0·01	15·6	16571	48·7	271	4·2
5	0·004	0·01	15·6	16706	5·2	268	14
5	0·004	0·01	15·6	11000	14·8	225	4
6	0·004	0·01	15·6	16000	15·2	273	1
7	0·004	0·01	15·0	15800	5·06	234	1
8	0·014	0·035	189	7734	28·2	261	14
8	0·014	0·035	190	18185	34	267	8
9	0·014	0·035	189	8537	10·2	261	11
9	0·014	0·035	192	15900	10	276	8
10	0·014	0·035	189	8790	10	261	4
10	0·014	0·035	192	16180	10	273	1

* The initial temperature obtained from the transient temperature data was always within 10 deg/F of T_0 (read by thermocouple).

DISCUSSION OF RESULTS

Mean wall temperature

A discussion of the present experimental model was given in [1]. The steady-state as well as the transient heat-transfer data have demonstrated that the flow in the test section (Fig. 2) simulates that of a flat plate in turbulent forced convection flow in the Reynolds number range $5 \times 10^5 \leqslant Re_L \leqslant 2 \times 10^6$. The use of the heated length of the ribbon L as the characteristic length proved satisfactory in [1] and will be followed here. Assumptions made in the analyses, (1) that the temperature is uniform across the thickness of the ribbon, (2) that the longitudinal conduction is negligible, and (3) that the heat generation is uniform along the ribbon, were shown [2] to be realistic for the present experimental model.

The test runs listed in Table 1 cover a Reynolds number range of $5 \times 10^5 \leqslant Re_L \leqslant 2 \times 10^6$. The periods of the exponential heat source t_0 were chosen to be characteristic of prompt critical excursions in water moderated reactors. The temperature–time histories of these runs are shown in Figs. 3–10 in terms of the dimensionless parameters Z_L/t_0, $t_0 u_\infty^2/\kappa$ and S; ($u_\infty = u_m/0{\cdot}8$), appearing in the turbulent solution in equations (15) and (16). All fluid properties are evaluated at the initial temperature of the fluid.

Where the heat source rises exponentially, as in the present case, there are two factors which mainly affect the heat-transfer process for a certain thermal capacity of the ribbon B^2 (note that $\sigma \cong 1$). These factors are the flow velocity u_∞ and the period of the exponential t_0. Different combinations of the velocity and the period may result in changes in the nature of the heat-transfer process. Over the ranges $1 \leqslant u_m \leqslant 14$ ft/s and $5 \leqslant t_0 \leqslant 50$ ms, the parameter $Z_L/t_0 = (L/u_\infty t_0)$ has been found to be a sufficient criterion in establishing ranges where the transient mean wall temperature can be satisfactorily predicted.

For small values of Z_L/t_0, $0{\cdot}28 \leqslant Z_L/t_0 \leqslant 2$, and for both wall thermal capacities listed in Table 1, the turbulent boundary-layer solution, equations (15) and (16), is shown in Figs. 3, 4, 8 and 9 to be in agreement with the experimental measurements for the mean wall temperatures. In these figures, the discrepancies between the turbulent solution and the experiments are, at all times, within the limits of probable experimental error. In this range of Z_L/t_0, the velocity and the period are usually large. The large velocity ensures that a turbulent boundary layer over the major portion of the ribbon is established. Moreover, the large period allows the temperature field to penetrate further in the turbulent hydrodynamic boundary layer. Note that for times t/t_0, which are comparable to Z_L/t_0, the convective cooling wave due to the velocity component u influences the entire

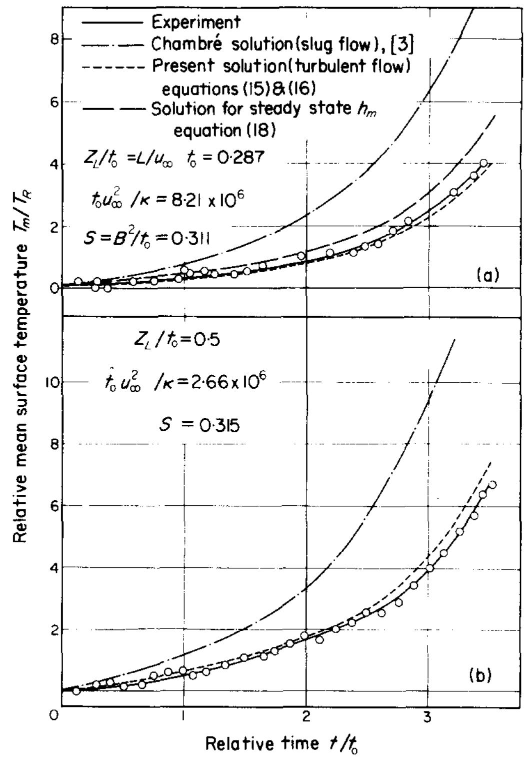

FIG. 3. Mean surface temperature response to an exponential rise in heat source ($Z_L/t_0 = 0{\cdot}287, 0{\cdot}5$).

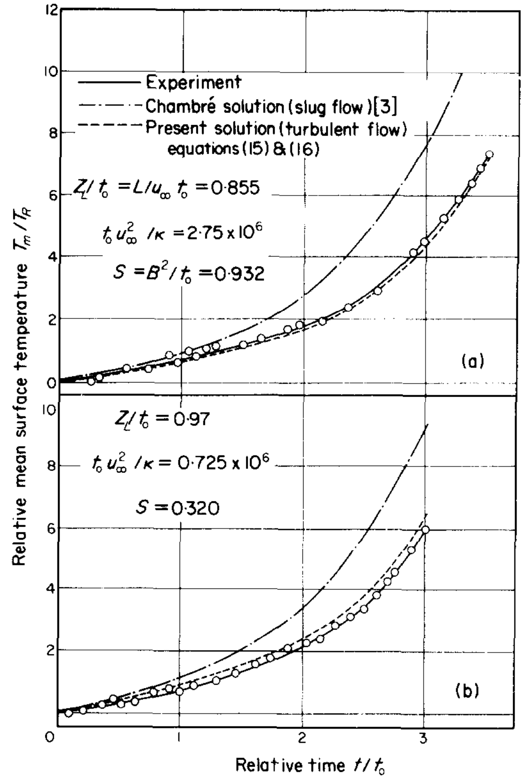

FIG. 4. Mean surface temperature response to an exponential rise in heat source ($Z_L/t_0 = 0{\cdot}855, 0{\cdot}97$).

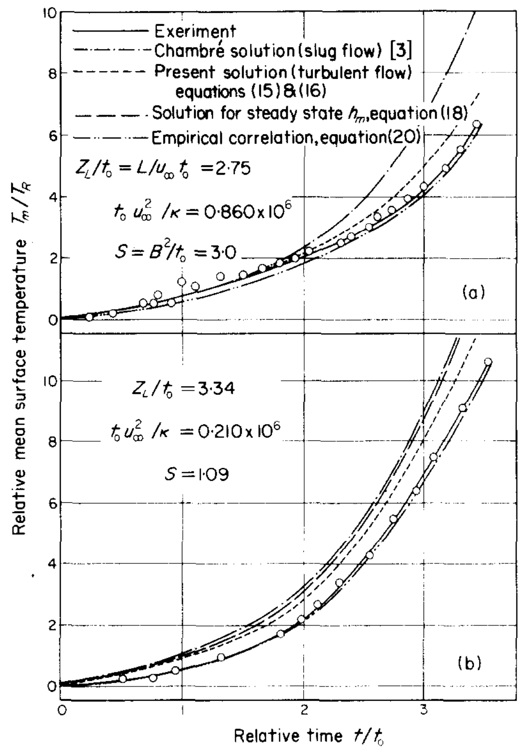

FIG. 5. Mean surface temperature response to an exponential rise in heat source ($Z_L/t_0 = 2{\cdot}75, 3{\cdot}34$).

length of the ribbon. Due to the factors mentioned above it should be expected that the Chambré slug flow solution [3, 4] overestimates the wall temperatures as exhibited by Figs. 3, 4, 8 and 9. For the same range of Z_L/t_0, the steady-state heat-transfer coefficient solution, equation (18), is found to lie above the turbulent boundary-layer solution. It is only shown in Figs. 3 and 8 to preserve the clarity of the rest of the figures. The deviation of this solution from the experimental data is within 20 degF. Since this solution is easier for numerical computations than equations (15) and (16), it is recommended for applications where a less accurate determination of the wall temperature is acceptable.

For large values of Z_L/t_0, $5 \leqslant Z_L/t_0 < \infty$, and also for both wall thermal capacities B^2 listed in Table 1, the Chambré slug flow solution is in agreement with the experimental data as shown in Figs. 6, 7 and 10. The differences between this solution and the measurements are also within the limits of probable experimental error. In this range of Z_L/t_0, both the flow velocity and the period are usually small. A small velocity indicates that a large portion of the hydrodynamic boundary layer is laminar. A short period means that the times involved are small and, hence, that the convective cooling wave, which is due to the velocity component u, has travelled only a short distance along the wall. These two factors cause the heat-transfer process to be more dominated by the one-dimensional molecular conduction. Consequently, Chambré solution predicts the measured wall temperatures satisfactorily while both the turbulent flow and constant h_m solu-

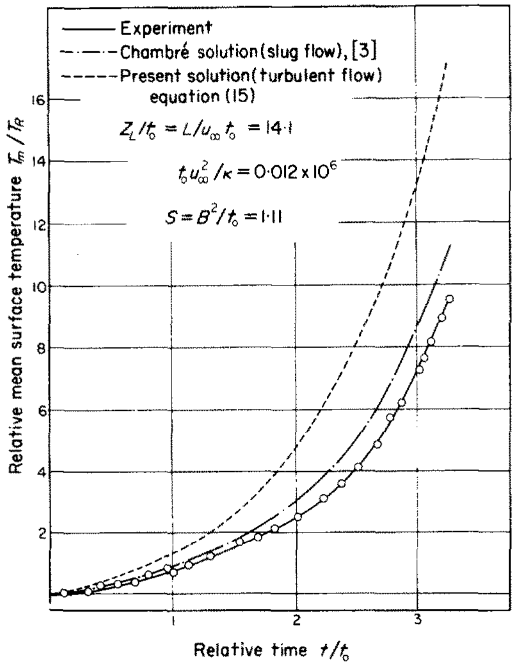

FIG. 6. Mean surface temperature response to an exponential heat source ($Z_L/t_0 = 14{\cdot}1$).

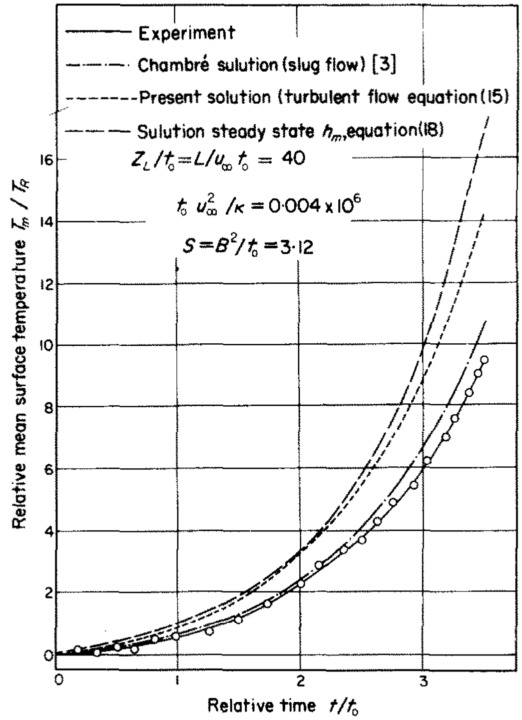

FIG. 7. Mean surface temperature response to an exponential heat source ($Z_L/t_0 = 40$).

tions overestimate the data in Figs. 6, 7 and 10. As Z_L/t_0 tends to infinity, (when $u_m \to 0$), the Chambré solution reduces to the conduction solution by Rosenthal and Miller, [8], which was in agreement with data taken with a similar ribbon mounted vertically in a pool of water.

For intermediate values of Z_L/t_0, $2 < Z_L/t_0 < 5$, both the turbulent flow and quasi-steady-state solutions as well as the Chambré solution overestimate the mean wall temperature as shown in Figs. 5 and 9. In this range of Z_L/t_0, the heat-transfer process becomes more complex and is not as well defined as in the two ranges of Z_L/t_0 previously discussed. A semiempirical correlation, based on the quasi-steady-state analysis, i.e. equation (18), is developed in the following paragraph for the determination of the mean wall temperature.

After examining the temperature data in this range of Z_L/t_0 to account for the lower temperatures revealed by the experiments, a new reduced value Z_L'/t_0 is defined as

$$Z_L'/t_0 = 0{\cdot}10\,(Z_L/t_0) \tag{19}$$

Substituting Z_L'/t_0 in place of Z_L/t_0 in equation (18) results in

$$T_m/T_R = \frac{\left\{\exp(t/t_0) - \exp\left[-0{\cdot}0627\,\frac{(t_0 u_\infty^2/\kappa)^{0\cdot 3}\,(t/t_0)}{(\sqrt{S})\,(Z_L/t_0)^{0\cdot 2}}\right]\right\}}{\left\{(\sqrt{S}) + 0{\cdot}0627\,\frac{(t_0 u_\infty^2/\kappa)^{0\cdot 3}}{(Z_L/t_0)^{0\cdot 2}}\right\}}. \tag{20}$$

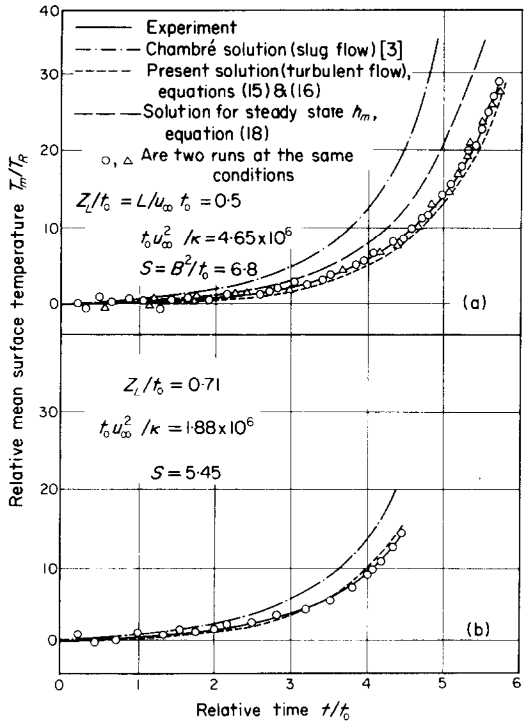

FIG. 8. Mean surface temperature response to an exponential heat source ($Z_L/t_0 = 0{\cdot}5$, $0{\cdot}71$).

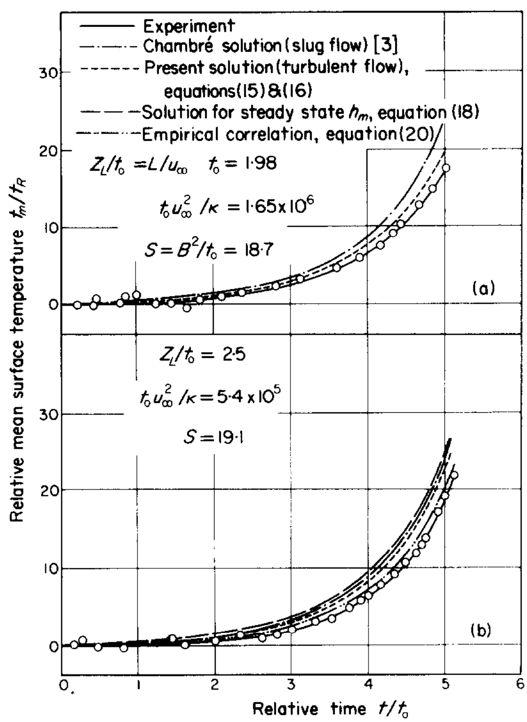

FIG. 9. Mean surface temperature response to an exponential heat source ($Z_L/t_0 = 1{\cdot}98$, $2{\cdot}5$).

Comparisons with the measured wall temperatures, demonstrate that equation (20) can satisfactorily predict the experimental data in the range $2 < Z_L/t_0 < 5$ and for both values of the wall thermal capacities listed in Table 1. Some typical comparisons are shown in Figs. 5 and 9.

Mean heat-transfer coefficient

The mean heat-transfer coefficient as defined in equations (5a) and (5b) is shown in Fig. 11 where T_m and $(\partial T_m/\partial t)$ are obtained from the measured temperature–time history. The test conditions shown in this figure are those of the thick ribbon and the highest flow velocity and period. For similar conditions except for a step heat source, h_m, as revealed by experiments and Chambré solution, was shown [1] to dip to a minimum before reaching the steady state. This dip was caused by the conjunction of a large wall thermal capacity and a sufficiently high flow velocity; it occurred at times $t > L/u_\infty$. However, the values of h_m shown in Fig. 11 do not exhibit any minimum. In view of equation (5a) and the explanation given in [1, 2], a minimum in h_m would be expected, in the present case, at times $t/t_0 > Z_L/t_0$ provided that the capacity term $H(\partial T_m/\partial t)$ is still significant. However, at these times the influence of the initial step q_0 has diminished and the capacity term is becoming smaller in comparison with the continuously rising source term. It is anticipated that for higher velocities and larger wall thermal capacities than those used in the present tests a minimum in h_m might be observed. This was revealed by examining h as predicted by Chambré solution (see [2]). The theoretical values of h_m obtained from the turbulent flow analysis, equations (11a) and (12a), are shown in Fig. 11 to be in agreement with the experimental h_m. Recalling that equations (11a) and (12a) are those of a wall of zero thermal capacity, it is feasible to conclude that the effect of the wall thermal

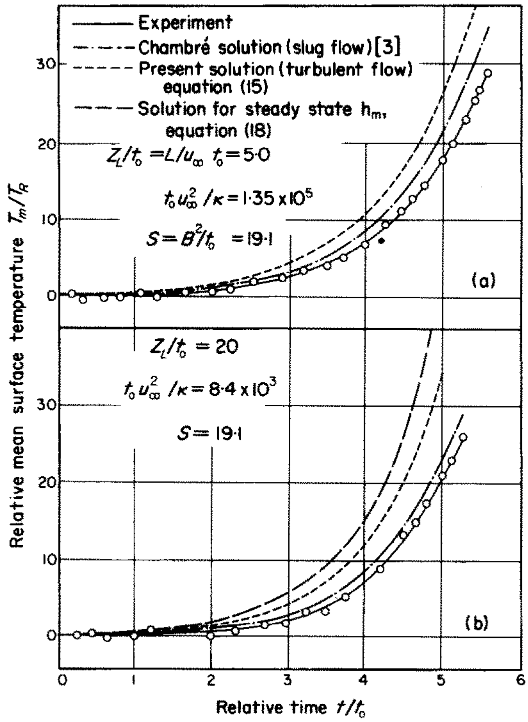

FIG. 10. Mean surface temperature response to an exponential heat source (Z_L/t_0 = 5, 20).

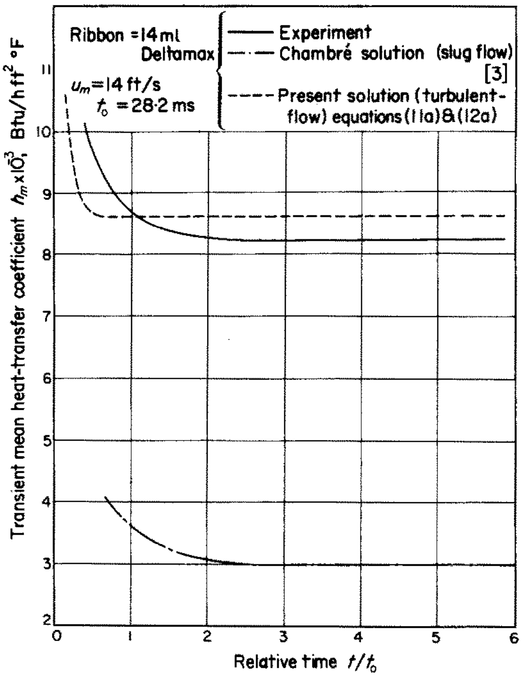

FIG. 11. Transient mean heat-transfer coefficient for 14 MIL Deltamax ribbon in case of an exponential heat source.

capacity on h_m is insignificant over the range of conditions covered in the present tests.

ACKNOWLEDGEMENT

This research was supported by the U.S. Atomic Energy Commission, Division of Reactor Development, Reactor Safety Branch, under Contract AT(11–1)–34 Project 42.

REFERENCES

1. M. SOLIMAN and H. A. JOHNSON, Transient heat transfer capacity and containing time-dependent heat source, *J. Heat Transfer*. To be published.
2. M. SOLIMAN, Analytical and experimental study of transient heat transfer for external forced convection, Ph.D. dissertation in Mechanical Engineering, University of California, Berkeley (January 1966); Also SAN 1011 Reactor Technology, TID 4500, 44 edn. (January 1966).
3. H. A. JOHNSON and P. L. CHAMBRÉ, Transient heat transfer for steady slug flow over a flat plate with uniform exponential heat generation, in *L. M. K. Boelter Anniversary Volume*. McGraw-Hill, New York (1964).
4. P. L. CHAMBRÉ, Theoretical analysis of the transient heat transfer into a fluid flowing over a flat plate containing internal heat sources, in *L. M. K. Boelter Anniversary Volume*. McGraw-Hill, New York (1964).
5. E. ECKERT and R. DRAKE, *Heat and Mass Transfer*, 2nd edn., p. 146. McGraw-Hill, New York (1959).
6. T. VON KÁRMÁN and M. A. BIOT, *Mathematical Methods in Engineering*, pp. 403–404. McGraw-Hill, New York (1940).
7. K. PEARSON, *Tables of the Incomplete Gamma Function*, pp. 118–127. Cambridge University Press, New York (1957).
8. H. A. JOHNSON, V. E. SCHROCK *et al.*, Temperature variation, heat transfer, and void volume development in the transient atmospheric (pool) boiling of water, University of California, Berkeley, IER Report Series 163, Issue No. 2 or SAN 1001, Reactor Technology TID 4500, 16th edn. (January 1961).

Résumé—On présente les résultats expérimentaux et les prévisions théoriques pour la température moyenne en régime transitoire de la paroi d'une plaque plane dont la capacité thermique est appréciable. Cette plaque est chauffée par une source de chaleur variant exponentiellement avec le temps (q_0 exp (t/t_0)) et refroidie des deux côtés par un écoulement de convection forcée, permanent et incompressible avec un nombre de Prandtl voisin de l'unité.

Dans la gamme de ces résultats, le paramètre $Z_L/t_0 = L/ut_0$ est un critère suffisant pour conclure que: lorsque $0{,}28 \leqslant Z_L/t_0 \leqslant 2$, une solution avec écoulement turbulent est en accord avec les resultats; est en bon accord avec les résultats; et lorsque $2 < Z_L/t_0 < 5$, on montre qu'une relation semi-empirique prédit la température pariétale d'une façon satisfaisante.

Zusammenfassung—Versuchsdaten und theoretische Berechnungen sind angegeben für die instationäre mittlere Wandtemperatur einer ebenen Platte grösserer Wärmekapazität, die von einer exponentiell wirkenden Wärmequelle ($q_0 \exp(t/t_0)$) beheizt und auf beiden Seiten von einer steten, inkompressiblen Zwangsströmung mit einer Prandtlzahl um 1 gekühlt wird. Im untersuchten Bereich stellt der Parameter $Z_L/t_0 = L/ut_0$ ein austeichendes Kriterium dar für folgende Schlussfolgerungen: für $0{,}28 \leqslant Z_L/t_0 \leqslant 2$ weist eine Lösung für turbulente Strömung gute Übereinstimmung mit den Werten auf: für $2 \leqslant Z_L/t_0 < \infty$ stimmt die Chambré-Lösung (slug Strömung) gut mit den Werten überein und für $2 < Z_L/t_0 < 5$ wurde eine halbempirische Korrelation entwickelt, die zufriedenstellend die Wandtemperatur wiedergibt.

Аннотация—Представлены экспериментальные и теоретические результаты для нестационарной температуры поверхности плоской пластины из материала с большой теплоемкостью, нагреваемой экспоненциальным источником тепла вида $q_0 \exp(t/t_0)$ и охлаждаемой с обеих сторон стационарным несжимаемым потоком вынужденной конвекции при числах Прандтля, близких с единице. В данном исследовании, параметр $L_L/t_0 = L/u\,t_0$ является критерием для того, чтобы сделать следующие выводы: при $0{,}28 \leqslant Z_L/t_0 \leqslant 2$ решение для турбулентного течения согласуется с экспериментальными данными; при $2 \leqslant Z_L/t_0 < \infty$ решение Шамбре (ползучее течение) хорошо согласуется с экспериментальными данными; для $2 < Z_L/t_0 < 5$ предложено полуэмпирическое соотношение, дающее удовлетворительные результаты для температуры стенки.